HHS Public Access

Author manuscript

Circulation. Author manuscript; available in PMC 2018 September 05.

Published in final edited form as:

Circulation. 2017 September 05; 136(10): 940–953. doi:10.1161/CIRCULATIONAHA.117.027889.

Interleukin 10 Inhibits Bone Marrow Fibroblast Progenitor Cell-mediated Cardiac Fibrosis in Pressure Overloaded Myocardium

Suresh Kumar Verma, Ph.D.[1,*], **Venkata N.S. Garikipati, Ph.D.**[1], **Prasanna Krishnamurthy, Ph.D.**[2], **Sarah M. Schumacher, Ph.D.**[1], **Laurel A. Grisanti, Ph.D.**[1], **Maria Cimini, BS.**[1], **Zhongjian Cheng, Ph.D.**[1], **Mohsin Khan, Ph.D.**[1], **Yujia Yue, B.S.**[1], **Cindy Benedict, Ph.D.**[1], **May M. Truongcao, B.S.**[1], **Joseph E. Rabinowitz, PhD.**, **David A. Goukassian, M.D.**[1], **Douglas Tilley, Ph.D.**[1,3], **Walter J. Koch, Ph.D.**[1,3], and **Raj Kishore, Ph.D.**[1,3,*]

[1]Center for Translational Medicine, Lewis Katz School of Medicine, Temple University, Philadelphia, Pennsylvania 19140 USA

[2]Department of Biomedical Engineering, School of Medicine, The University of Alabama at Birmingham Alabama 35294 USA

[3]Department of Pharmacology, Lewis Katz School of Medicine, Temple University, Philadelphia, Pennsylvania 19140 USA

Abstract

Background—Activated fibroblasts (myofibroblasts; myoFBs) play critical role in cardiac fibrosis; however, their origin in the diseased heart remains unclear warranting further investigation. Recent studies suggest the contribution of bone marrow fibroblast progenitor cells (BM-FPC) in pressure overload (PO)-induced cardiac fibrosis. We have earlier shown that interleukin-10 (IL10) suppresses PO-induced cardiac fibrosis; however, the role of IL10 in inhibition of BM-FPC-mediated cardiac fibrosis is not known. We hypothesized that IL10 inhibits PO-induced homing of BM-FPCs to the heart and their trans-differentiation to myoFBs and thus attenuates cardiac fibrosis.

Methods—Pressure overload was induced in wild-type (WT) and IL10 knockout (IL10KO) mice by transverse aortic constriction (TAC). To determine the bone marrow origin, chimeric mice were created using eGFP WT mice marrow to the IL10KO mice. For mechanistic studies, fibroblast progenitor cells were isolated from mouse bone marrow.

Results—Pressure overload enhanced bone marrow fibroblast progenitor cell (BM-FPC) mobilization and homing in IL10KO mice compared to WT mice. Furthermore, WT bone marrow (from eGFP mice) transplantation in BM-depleted IL10KO mice (IL10KO chimeric mice) reduced TAC-induced BM-FPC mobilization compared to IL10KO mice. GFP co-staining with αSMA or collagen 1α in left ventricular tissue sections of IL10KO chimeric mice suggest that myofibroblasts were derived from bone marrow post-TAC. Finally, WT-BMT in IL10KO mice inhibited TAC-induced cardiac fibrosis and improved heart function. At the molecular level, IL10

[*]Address Correspondence to: Raj Kishore, PhD and/or Suresh K Verma, PhD (@MasterIshan), Lewis Katz School of Medicine,, 3500 N. Broad Street, MERB-954, Temple University, Philadelphia 19140, Tel: 215-707-2523, Fax: 215-707-9890, raj.kishore@temple.edu (RK), suresh.verma@temple.edu (SKV).

Disclosures: None

treatment significantly inhibited TGFβ-induced transdifferentiation and fibrotic signaling in WT BM-FPC in vitro. Furthermore, fibrosis-associated miRNAs expression was highly upregulated in IL10KO-FPCs compared to WT-FPCs. PCR-based selective miRNA analysis revealed that TGFβ-induced enhanced expression of fibrosis-associated miRNAs (miRNA-21, -145 and -208) was significantly inhibited by IL10. Restoration of miRNA-21 levels suppressed the IL10 effects on TGFβ-induced fibrotic signaling in BM-FPC.

Conclusion—Our findings suggest that IL10 inhibits BM-FPC homing and trans-differentiation to myofibroblasts in pressure overloaded myocardium. Mechanistically for the first time we showed that IL10 suppresses Smad-miRNA-21 mediated activation of BM-FPCs and thus modulates cardiac fibrosis.

Keywords

Cardiac fibrosis; Bone marrow progenitor cells; Heart failure; Inflammation; miRNAs

Introduction

Heart failure is the leading cause of morbidity and mortality in the developing world [1]. A key component of heart failure is excessive extracellular matrix deposition by activated fibroblasts (myofibroblasts; myoFBs); this leads to cardiac fibrosis and pathological remodeling in myocardium [2–4]. Myofibroblasts play a prominent role in fibrotic processes and display unique biological functions including increased production of fibrillar type I and III collagen [3, 5–7]. Myofibroblasts also express high levels of the contractile protein α-smooth muscle actin (αSMA), by which they can exert strong contraction forces, thereby reducing the damaged area [5, 8, 9]. In contrast, dysregulated activation of cardiac fibroblasts and their secreted cytokines and growth factors, such as TGFβ and endothelin, enhances hypertrophic cardiac remodeling and ultimately leads to heart failure.

In general, healthy myocardium does not contain myofibroblasts. The origin of the myofibroblasts responsible for the excessive collagen and other extracellular matrix protein production in a pressure overload (PO)-induced hypertrophic model has not been entirely elucidated. During development, cardiac fibroblast originates from mesenchymal cells primarily derived from the embryonic epicardium [10, 11]. It was previously thought that this source of mesenchymal cells does not persist into adulthood [12, 13]. However, mesenchymal stem cells have been found to significantly contribute in the wound healing process post-MI [14]. Previous studies have shown that myofibroblasts may originate from several sources, including expansion of resident fibroblasts, hematopoietic cells mobilized from bone marrow [12, 15–17], or from endothelial cells by the process of endothelial to mesenchymal transition (EndoMT) [18, 19]. Recent studies suggest that a subpopulation of heart-infiltrating BM-derived $CD45^+$ cells expressing prominin 1 and other stem cell markers (such as cKit and Sca1), contribute to myoFB differentiation under the influence of pro-fibrotic factors TGFβ [15, 20, 21]. Nonetheless, although it is now more widely accepted that there are other sources of myoFB beyond resident cardiac fibroblasts, there is still debate about the extent to which these extra-cardiac cells contribute to cardiac fibrosis thus warranting further investigation [22–24].

MicroRNAs (miRNAs) are noncoding single-stranded RNAs (approximately 18–24 nucleotides in length) and are involved in post-transcriptional control of genes. Recently, they have emerged both as key regulators of cardiovascular disease and as potential drug targets [25, 26]. Emerging evidence suggests a pivotal role for miRNAs in cardiac fibroblast proliferation and differentiation [26, 27]. Interestingly, it has been demonstrated that TGFβ-Smad signaling plays a critical role in regulation of miRNA-21 biogenesis in vascular smooth muscle cells [28, 29]. Furthermore, in vivo silencing of miRNA-21 suppresses TGFβ-induced non-canonical (ERK-MAP kinase) fibrotic signaling and prevents cardiac dysfunction in mouse after transverse aortic constriction [30]. miRNA-21 regulates fibroblast survival and growth factor secretion, which ultimately control the extent of cardiac fibrosis and hypertrophy [30, 31]. However, the role of miRNA-21 in BM-FPC trans-differentiation and in BM-FPC-mediated fibrosis has never been studied.

Interleukin-10 (IL10) is a pleiotropic cytokine that regulates the infiltration of monocytes/macrophages to the injured site and controls the synthesis of various pro-inflammatory cytokines and chemokines [32, 33]. IL10 therapy has been successfully tried in a variety of inflammatory diseases including myocardial infarction (MI) and ischemic injury [33, 34]. Recently we have shown that recombinant mouse lL10 treatment significantly inhibits local cytokine expression and subsequently attenuates pressure overload-induced inflammation and hypertrophic remodeling [32]. In fact, IL10KO mice showed exaggerated fibrosis and IL10 treatment resulting in attenuated left ventricular fibrosis in multiple heart failure models (aortic banding, isoproterenol, Ang II and myocardial infarction) [32, 34, 35]. However, molecular mechanisms for the anti-fibrotic effect of IL10 are not known. Others and we have shown that IL10 regulates trafficking of bone marrow stem/progenitor cells to the heart; however, the role of IL10 in homing of bone marrow fibroblast progenitor cells (BM-FPCs) to the heart and the contribution of IL10 to pathological fibrosis has never been studied.

In this study, we tested the hypothesis that IL10 inhibits bone marrow-derived myofibroblast-mediated cardiac fibrosis and improves cardiac function in the pressure-overloaded myocardium. We report that TAC-induced mobilization and homing of BM-FPCs to the heart is augmented in IL10 KO mice. Wild type bone marrow cell transplantation into IL10KO mice markedly reduced mobilization of BM-FPCs and reduced TAC-induced cardiac fibrosis. Furthermore, IL10 suppressed TGFβ/Smad signaling induced miRNA-21 expression. The regulation of miRNA-21 expression by IL10 in activated BM-FPCs could be a potential mechanism by which IL10 reduces fibrosis in the pressure-overloaded myocardium.

Materials and Methods

Antibodies and reagents

Antibodies against α-smooth muscle actin (αSMA), collagen 1α or FSP1 (Fibroblast specific protein1) were purchased from Abcam, Inc. (San Francisco, California). Antibodies specific for pSmad2/3, total-Smad or GAPDH were purchased from Cell Signaling Technology, Inc. (Boston, MA). For cell purification, prominin 1, and CD45 antibodies were purchased from EMD Millipore, Inc. (Billerica, MA). PE-Prominin 1, FITC-CD45 antibodies were purchased from Miltenyi Biotec, Inc. and BD Pharmingen Inc. respectively.

For cell treatments, recombinant murine IL10 and TGFβ were obtained from R&D Systems, Inc. (Minneapolis, MN).

Animals and surgeries

The Institutional review Board (IRB) approval was obtained from the institutional biosafety committee of Temple University. All animal experiments adhered to the protocols approved by the Institutional Animal Care and Use Committee of Temple University. Eight- to ten-weeks old wild-type (WT C57BL/6J) and IL10-KO (IL10KO; $Il10^{tm1Cgn}$) mice were procured from Jackson Research Laboratory (Bar Harbor, ME). Male transgenic eGFP-expressing (C57BL/6-Tg[CAG-EGFP]10sb/J) mice served as a donor source in bone marrow transplantation (BMT) experiments. Before surgery, baseline echocardiography data were collected for all animals. Cardiac hypertrophy and subsequent heart failure were induced by constriction of the transverse aorta using a 27G needle as described previously [32, 36].

Isolation of prominin 1 positive cells and treatments

Prominin 1 positive cells (BM-FPCs) were isolated from bone marrow of both WT and IL10KO mice using prominin 1 and CD45 magnetic bead double-selection method. BM-FPCs were isolated from bone marrow mononuclear cells using density-gradient centrifugation as described previously [34]. Briefly, bone marrow cells were isolated from both fore and hind limbs. For positive cell separation, monocyte/macrophage-depleted bone marrow cells were incubated with prominin 1 magnetic bead for 25–30 min. After serial washing steps, the cells were cultured in expansion medium (IMDM with 20% FBS, 100 μM β-mercaptoethanol, 1% non-essential amino acids, and 1% antibiotic/antimycotic (Mediatech). 10–12 days after culture, cells were detached using trypsin (0.05% with EDTA) and CD45-positive progenitor cells were sorted from expanded total prominin 1-positive cells using CD45-magnetic beads. The sorted prominin 1+CD45+ cells were plated on 1% gelatin-coated plates in expansion medium till confluency. For *in vitro* experiments, cells were starved in serum-free medium (SFM) for 12 hours. BM-FPCs were pre-treated with IL10 (20 ng/ml) for one hour followed by TGFβ (20 ng/ml) for 6 (protein analysis), 24 (RNA analysis) or 72 (immunostaining) hours.

Bone marrow transplantation and surgery

To elucidate the role of IL10 in BM-FPC homing to the heart, we conducted BM transplantation (BMT) experiments using eGFP-transgenic mice as BM donors as described previously [34]. For BMT, recipient female IL10-knockout (KO) mice (5 weeks old) were lethally irradiated with a 6.0 Gy dose followed by intravenous injection of 2×10^6 donor BM cells isolated from male donor eGFP+ WT mice. At 5 weeks after BMT, recipient IL10KO chimeric mice were subjected to TAC surgery as described previously [32, 36]. At day 5, TAC-induced mobilization of BM-FPCs was determined by FACS analysis of peripheral blood mononuclear cells. On day 28, after final echocardiography, mice were euthanized and heart was isolated for biochemical analysis.

Tissue Preparation and Flow Cytometry

Flow cytometry analysis of BM-FPCs population was performed on cells isolated from blood and heart as described previously [34]. Blood was collected into EDTA-containing tubes either via tail vein cut (from live mice) or via cardiac rupture (from euthanized mice). Whole blood was stained with fluorochrome-conjugated antibodies (CD45-FITC and prominin1-PE), and erythrocytes were then lysed using BD FACS lysis solution (BD Biosciences). After blood collection, hearts were perfused with EDTA supplemented Hank's Balance Salt Solution (HBSS) and chopped in small pieces. For single cell preparation, the chopped heart pieces were digested using mixture of collagenase D and DNase I (both from Roche) in HBSS at 37°C for 40 min and filtered through 70-μm nylon mesh. Erythrocytes were lysed using BD Pharm Lyse (BD biosciences), and counted with trypan blue to discriminate the dead cells. The freshly isolated heart or mononuclear cells from peripheral blood (tail vein) were separated with antibodies against CD45-FITC (BD Pharmingen Inc.) and prominin1-PE (Miltenyi Biotec, Inc.) and sorted on an LSRII flow cytometer for size and granularity by forward scatter and side scatter. Isotype-matched IgG antibodies were used as negative controls. Quantitative fluorescence analysis was performed with Flow-Jo Software (Tree Star, Inc.); 50,000 events were counted per sample.

Cardiac imaging

Transthoracic two-dimensional M-mode echocardiography was performed using a Vevo 770 (VisualSonics, Toronto, Canada) equipped with a 30 MHz transducer. Echocardiographic studies were performed before (baseline) and at 28 days post-surgery. Percent fractional shortening (% LVFS) and % ejection fraction (%LVEF) was calculated as described previously [34, 37, 38].

Tissue preparation & Masson's trichrome staining

Whole hearts were perfused first with sterile cold PBS followed by 10% formalin for 5–10 min. Atria were removed and ventricles were fixed in 10% phosphate buffered formalin for 24 hours. 20–25 sections (4 μm each) were prepared from each heart and MT staining and quantification were done using Nikon NIS software [32].

Quantitative real-time PCR

Gene expression levels of collagen1α, TGFβ, αSMA and FSP1 were quantified in the prominin 1^+ fibroblasts progenitor cells as described previously [32]. RNA was collected with Trizol RNA isolation kit. Total RNA was reverse transcribed with iScript cDNA Synthesis Kit (Bio-Rad Laboratories, Hercules, CA), and amplification was performed using a Taqman 7700 (Applied Biosystems, Foster City, CA). Relative mRNA expression of target genes was normalized to the endogenous 18S control gene (Applied Biosystems, Foster City, CA) and represented as fold-change *vs.* respective controls.

miRNA expression analysis

PCR-based miRNA array was performed to measured the levels of fibrosis-associated miRNA in BM-FPCs as per manufacturer's instructions (RT2 Profiler; SABiosciences) [35]. Briefly, total RNA was collected with using Trizol RNA isolation kit (Qiagen). Total RNA

was reverse transcribed with provided cDNA Synthesis Kit (Qiagen), and amplification was performed using a StepOnePlus (Applied Biosystems, Foster City, CA). Relative expression of target miRNAs was normalized to the endogenous U6 control gene (Applied Biosystems, Foster City, CA) and represented as fold-change *vs.* respective controls.

Preparation of cell lysates and western blotting

Fibroblast progenitor cells were lysed in RIPA cell lysis buffer (Cell Signaling, Boston, MA) supplemented with protease inhibitor pellets (Amersham Biosciences, Piscataway, NJ). Insoluble debris was removed by centrifugation (25,000 g) for 15 min at 4°C and cell lysates were boiled with Laemmli sample buffer (0.5 mol/L Tris-HCl [pH 6.8], 10% SDS, 10% glycerol, 4% β-merceptoethenol and 0.05% bromophenol blue). Equal amounts of protein (20μg) were separated by SDS-PAGE and assessed by western blotting in indicated protein(s). GAPDH was used as a loading control [39].

Immunofluorescent staining

Immunofluorescent staining for prominin 1, collagen 1α, FSP1 and α-SMA was performed on tissue sections or on fibroblast progenitor cells plated onto chamber slides coated with 1% gelatin. BM-FPCs were grown to ~80% confluence (5–7 days) in culture expansion media. The medium was changed to serum-free IMDM for treatment. Prior to immunostaining, cells were washed with PBS and fixed in 4% PFA for 15 min and permeabilized for 10 min using 0.2% Triton® 100. BM-FPCs were incubated for 1 h (22°C) with blocking solution (3% bovine serum albumin, 10% horse serum and 0.2% Triton X-100) to block nonspecific binding. Cells were then incubated at 37°C for 1 h with primary antibodies and 45 min with the appropriate secondary antibody conjugated to Alexa-488 or Alexa 594 (Invitrogen). DAPI was used to counterstain the nuclei. Cells were covered with mounting medium (Invitrogen), overlaid with a coverslip and examined under a fluorescence microscope. For tissue sections, all the steps are identical following the de-paraffinization steps [39].

Statistical Analysis

Results are expressed as the mean ± standard error of the mean (SEM), computed from separate experiments. Comparisons of continuous variable between treatment groups were performed with the nonparametric Kruskal-Wallis test for 3 or more groups (level of significance were determined by Dunn’s nonparametric test) and the exact Wilcoxon rank sum test for 2 groups because of the small group sizes to guard against possibly non-normally distributed data. When data were collected over time on the same set of animals such as % fractional shortening and % ejection fraction, they were analyzed with a mixed-effects model to take into account the correlation among repeated measures and the potential nonconstant variability over time across different groups. Multiple comparisons among treatment groups were performed using one-way or two-way repeated analysis of variance (ANOVA) and levels of significance were determined using the Tukey-Kramer multiple comparison post-hoc test. The statistical analysis was performed using GraphPad Prism 6.0h software Inc., San Diego, CA). P values <0.05 were considered to be statistically significant. P values and n (group size) values are reported in the figure legends.

Results

Augmented TAC-induced mobilization and homing of fibroblast progenitor cells in IL10 KO mice

To investigate whether IL10 regulates TAC-induced mobilization and homing of fibroblast progenitor cells (BM-FPCs) to the heart, we evaluated BM-FPC mobilization and homing in WT and IL10 KO mice 5 days after TAC surgery by FACS. BM-FPCs were identified as the subpopulation of lineage negative hematopoietic cells (CD45+) expressing prominin 1 as described previously [15, 21]. As shown in Figure 1A, TAC significantly induced BM-FPC mobilization from bone marrow to the peripheral blood in both WT and IL10KO mice; however, the TAC-induced circulating BM-FPC number was augmented in IL10KO mice. Furthermore, to assess the homing of BM-FPCs to the heart; FACS was performed in the enzyme-digested WT and IL10KO mice hearts cells from WT and IL10KO mice 5 days after TAC surgery. An increased number of BM-FPCs were detected in the WT hearts post-aortic constriction, as compared to hearts from sham-operated WT mice. PO-induced recruitment of BM-FPCs into the heart was further augmented in IL10 KO mice (Figure 1B).

IL10 inhibits TGFβ-induced trans-differentiation of BM-FPCs to myoFBs

BM-FPCs were isolated from bone marrow of WT mice. To induce BM-FPC trans-differentiation, cells were treated with TGFβ (20ng/ml) in the presence or absence of IL10 (20ng/ml). At the end of the treatment, cells were washed with cold PBS, fixed in 4% PFA (15 min) and stained with αSMA (myoFB marker) and prominin 1 (Figure 2A–D). TGFβ treatment enhanced αSMA expression in BM-FPCs (Figure 2C). Furthermore, TGFβ-treated cells also showed myofibroblast (myoFB)-like spindle shape morphology. TGFβ-induced αSMA expression and morphological change were markedly inhibited by IL10 treatment (Figure 2D–E), suggesting that IL10 inhibits TGFβ-induced BM-FPC trans-differentiation to myoFB.

TGFβ-induced fibrotic gene expression was inhibited by IL10

To define the myofibroblast phenotype in TGFβ-treated cells, we measured the expression of fibroblast-associated genes [TGFβ (**A**), collagen1α (**B**), FSP-1 (**C**) and αSMA (**D**)] by quantitative RT-PCR. TGFβ treatment significantly enhanced fibrosis-associated gene expression in BM-FPCs (Figure 3A–D). Interestingly, TGFβ-induced fibrosis-associated gene expression was reduced by IL10 treatment (Figure 3A–D). These data further substantiate that IL10 inhibits BM-FPC trans-differentiation to myoFB.

IL10 inhibits TGFβ signaling in bone marrow fibroblast progenitor cells

To understand the effect of TGFβ treatment on myofibroblast-related protein expression and signaling, we measured the αSMA protein levels in cell lysates isolated from fibroblast progenitor cells after IL10 and/or TGFβ treatments. TGFβ significantly increased αSMA protein levels in BM-FPCs; conversely, this increase was inhibited by IL10 treatment (Figure 3E–F). This result further confirms that IL10 inhibits BM-FPC trans-differentiation. Furthermore, to determine the contribution of TGFβ downstream signaling molecule on

BM-FPC trans-differentiation, western blot for pSmad2/3 was performed in whole cell lysates from BM-FPCs after TGFβ and/or IL10 treatment. TGFβ strikingly increased Smad2/3 phosphorylation and, corroborating our other results, Smad2/3 phosphorylation was markedly reduced by IL10 treatment (Figure 3E&G).

Reconstitution with WT bone marrow in irradiated IL10KO mice prevents BM-FPC mobilization and homing

To further elucidate the role of IL10 on BM-FPC mobilization, we conducted BM transplantation (BMT) experiments using eGFP-transgenic mice as bone marrow donors for IL10KO recipients, five weeks prior to TAC surgery. At 5 days post-TAC, numbers of BM-FPCs were measured by FACS in peripheral blood obtained from WT, IL10KO and IL10KO chimeric mice. TAC-induced mobilization of BM-FPCs in IL10KO mice was partially diminished by WT bone marrow transplantation (Figure 4A–E). This result suggests that reconstitution with WT bone marrow cells in IL10KO mice is sufficient to restrict the release of BM-FPCs from bone marrow.

Bone marrow fibroblast progenitor cells trans-differentiate into myofibroblasts in pressure-overloaded myocardium

To evaluate whether fibroblast progenitor cells homed into the heart, 5 days after TAC, left ventricular sections from IL10KO chimeric (eGFP-WT bone marrow recipient) mice examined by immunofluorescence microscopy for GFP and prominin 1 expression. Our data demonstrate that TAC induced recruitment of WT bone marrow progenitor cells to the heart (Figure 5A–B). GFP-prominin 1+ double positive cells (yellow) were noticeably detectable in chimeric mouse hearts 5 days after TAC. These results confirm that pressure overload significantly enhances recruitment of bone marrow fibroblast progenitor cells to the heart (Figure 5B). Furthermore, to study the contribution of these cells to cardiac fibrosis, 28 days after TAC, left ventricular sections from chimeric IL10KO mice were examined for co-expression of GFP and αSMA (myofibroblast marker). Due to reduced BM-FPC mobilization in sham mice, very little GFP positive cells were seen. Interestingly, TAC induction resulted in a notable increase in double-positive cells and those co-expressing GFP and αSMA (Figure 5C–D). The presence of double-positive cells suggest that bone marrow progenitor cells in the failing hearts trans-differentiated to myofibroblasts (yellow). To further validate the myoFB phenotype, LV sections were examined for the myofibroblast marker procollagen 1α (red) co-expressed with GFP with similar results (supplementary Figure S1).

WT bone marrow reconstitution in IL10 KO mice partially reduced cardiac fibrosis and improved cardiac function in the pressure-overloaded myocardium

As WT bone marrow transplantation noticeably reduced the mobilization of fibroblast progenitors, we next assessed whether reduced fibroblast progenitor cell homing affects cardiac fibrosis in the chimeric IL10KO mice post-TAC. Masson's trichrome staining was performed to see the collagen deposition in the heart sections. As expected, IL10KO mice showed exaggerated fibrosis compared to WT mice post-surgery (Figure 6A–D). WT bone marrow transplantation in IL10KO mice significantly attenuated TAC-induced exaggerated fibrosis (Figure 6C–D). Furthermore, cardiac function was measured on baseline, 15 and 28

days post-aortic constriction by echocardiography. Cardiac function was greatly impaired in IL10KO mice as compared to WT mice post-surgery. Intriguingly, WT bone marrow-transplantation in IL10KO chimeric mice significantly improved heart function (Figure 6E–F).

TGFβ augments fibrosis-associated miRNA expression in IL10KO-derived fibroblast progenitor cells

To understand the underlying mechanisms of TGFβ-induced fibroblast progenitor cell trans-differentiation, we performed a series of *in vitro* experiments in isolated fibroblast progenitor cells. As miRNAs control a wide range of physiological/pathological processes including pro-fibrotic signaling [25, 26], we assessed the role of miRNAs on BM-FPCs trans-differentiation and whether IL10 regulates their expression. Fibrosis-associated miRNA expression was analyzed in WT and IL10 KO BM-FPCs at basal level using a PCR-based miRNA microarray platform (Qiagen). miRNA-array data showed that several miRNAs were differentially expressed in IL10KO BM-FPCs compared to WT BM-FPCs (Figure 7A). Among these, miRNA-21, -145 and -208a were highly up-regulated in IL10 KO BM-FPC compared to WT BM-FPC. Furthermore, to determine whether TGFβ treatment induces miRNAs -21, -145 and -208a expressions and IL10 treatment inhibits TGFβ-induced miRNAs expression, miRNA-21, miRNA-145 and miRNA-208a expression was measured in WT-FPCs after TGFβ or with TGFβ and IL10 treatments by qRT-PCR. TGFβ treatment significantly increased miR-21, -145 and -208a expression in WT cells (Figure 7B–D). The TGFβ-induced miR -21/-145/-208a expressions were significantly attenuated by IL10 treatment (Figure 7B–D). These results suggest that miRNA-21/-145/-208a play important role in TGFβ-induced BM-FPC's trans-differentiation and IL10 negatively regulates their expression.

miR-21 overexpression attenuates IL10 effect on TGFβ-induced BM-FPC trans-differentiation

Previous studies have suggested a significant role of miRNA-21 in TAC-induced cardiac fibrosis [30]. To determine whether IL10 negatively regulates miR-21 expression and thus inhibits BM-FPC trans-differentiation, WT BM-FPCs were transfected with miR-21 mimic and respective control scrambled RNA. miRNA-21 mimic transfection significantly increased miRNA-21 expression level in BM-FPCs (Figure 8A). Furthermore, fibrosis-associated gene expression was also measured in miRNA-21 mimic-treated cells after IL10 and/or TGFβ treatment. TGFβ-induced fibrotic gene (TGFβ, Col1α, Col3α and FSP-1) expression was augmented in miRNA-21 mimic-treated cells (Figure 8B–E). Moreover, the inhibitory effect of IL10 on TGFβ-induced fibrotic genes expression was almost completely ablated by miRNA-21 overexpression (Figure 8B–E). These results demonstrate that the inhibitory effect of IL10 on TGFβ-induced BM-FPC trans-differentiation is miRNA-21-dependent.

Discussion

Fibrosis is an evolutionarily conserved process that serves to facilitate host defense and wound healing. Deregulated fibrosis, however, is invariably associated with loss of organ

function. For instance, cardiac fibrosis is correlated with elevated mortality in dilated cardiomyopathy, which is the most common cardiomyopathy globally and directly correlates with sudden cardiac death, heart failure and arrhythmia [12]. Despite significant progress made in identifying molecular mechanisms and/or factors that contribute to hypertrophy over the past decades, the mechanistic basis of cardiac fibrosis is still not well understood. This study demonstrates that in addition to resident cardiac fibroblasts, bone marrow-derived fibroblasts significantly contribute to progression of pathological cardiac fibrosis and remodeling, and that pleotropic anti-inflammatory cytokine IL10 inhibits the recruitment and trans-differentiation of BM-FPCs into the pressure-overloaded myocardium. Furthermore, we show that IL10 noticeably inhibits TGFβ-Smad2/3 signaling in activated BM-FPCs. We reported the suppression of TGFb-Smad2/3 signaling-mediated miRNA-21 maturation as a novel mechanism by which IL10 might potentially inhibit BM-FPC-mediated cardiac fibrosis in the pressure-overloaded myocardium.

Structural fibroblasts are considered as one of the most abundant cell types in the adult myocardium, which perform structural function and also provide the source of continued renewal of matrix proteins [4]. Although cardiac fibroblasts are highly active during organ development, cardiac fibroblasts of the adult heart are quiescent and maintain only a low-level turnover of ECM [5]. In response to tissue injury (including mechanical, ischemic or inflammatory), fibroblasts are activated, become myofibroblasts, and are involved in active matrix deposition and tissue fibrosis. Recent evidence suggests that the overall number of myofibroblasts in the injured myocardium is rapidly increased due to proliferation of existing fibroblasts and of trans-differentiation from bone marrow hematopoietic cells, endothelial cells or epicardial cells [16]. Recent literature advocate that a subpopulation of heart-infiltrating BM-derived $CD45^+$ cells, expressing prominin 1 and other stem cell markers (c-Kit and Sca-1), contribute to cardiac fibrosis under the influence of TGFβ [15, 20, 21]. These cells are common progenitors for fibroblasts and macrophages. The inflammatory stimulus (M-CSF) induced their differentiation to macrophages; however, fibrotic stimuli (TGFβ) induced their differentiation to myofibroblasts. In sex-mismatched bone marrow transplantation experiments, Zeisberg et al. have shown that almost 21% of myofibroblasts are derived from the bone marrow in fibrotic lesions after pressure overload [18]. In agreement with these data, we also found that pressure overload enhances mobilization and homing of CD45/prominin1 positive cells to the heart. Interestingly, the mobilization of cells from this source was further augmented in IL10 knockout mice. Our result suggests that IL10 negatively regulates the homing of BM-FPCs to the heart. This notion was further confirmed in our bone marrow transplantation experiments where transplantation of WT bone marrow in IL10KO chimeric mice partially reduced BM-FPC mobilization after TAC. Acute inflammatory stimulus during myocardial infarction leads to release of hematopoietic and mesenchymal stem cells from bone marrow and to their recruitment to the heart [40, 41]. Although the primary role of bone marrow cells (including monocytes/macrophages, endothelial cells or other mesenchymal cell) trafficking to the heart is cardiac repair, but a prolonged inflammatory state leads to adverse remodeling and cardiac cell death [42]. Therefore, a tight regulation of inflammation is indeed important for adequate cardiac repair during inflammation-associated heart disease. Others and we have previously shown that IL10 attenuated both MI and PO-induced inflammation in mouse

heart and improved cardiac function [32, 33, 37]. As inflammatory stimuli play an important role in the bone marrow microenvironment and biology of bone marrow cells, the reduced mobilization of fibroblast progenitor cells in IL10 KO chimeric mice in this study could be due to changes in the bone marrow microenvironment (due to WT bone marrow cell transplantation).

In the past years, regeneration of ischemic myocardial tissue has been attempted using bone marrow-derived stem cells (BMCs) and wide variety of stem cells As an alternative to the direct intramyocardial injection, mobilization of BMCs using growth factors, such as the hematopoietic cytokine granulocyte-colony stimulating factor (G-CSF) or even IL10, have been successfully utilized [34, 43]. Migration of circulating mobilized BMCs from the bloodstream into the damaged tissue is suggested to play a key role for tissue regeneration. In fact, recently we have shown that homing of endothelial progenitor cells is important for adequate cardiac repair post-MI. The compromised bone marrow environment in IL10 KO mice leads to impaired release of EPCs from bone marrow [34]. Interestingly, in contrast to BM-EPCs, IL10KO mice bone marrow facilitates the homing of fibroblasts progenitor cells to the heart post-TAC in this study. Our data indicates that IL10 has differential effects on the release of subsets of bone marrow cells. The differential effect of IL10 on release of bone marrow subsets could be the long-term chronic heart failure model used in current study.

It is well established that TGFβ enhances the transition from acute inflammatory phase to chronic fibrotic phase during pathological heart disease [15, 44]. We have previously shown that IL10 knockout mice showed exaggerated TGFβ gene expression within 7 days in pressure overloaded myocardium, which ultimately led to exaggerated cardiac fibrosis [32]. In the present study, we found that the BM-FPCs are recruited to the heart mostly after 5–7 days post-surgery (Figure 5A–B). Kania et al has recently shown that blockade of TGFβ signaling using TGFβ neutralizing antibody inhibits trans-differentiation of bone marrow prominin 1 positive cells to myofibroblasts [15, 20]. Thus the augmented fibrotic response of pressure overload in IL10 KO mice could be due to enhanced recruitment and trans-differentiation (in the presence of TGFβ) of BM-FPCs. Interestingly, the TGFβ-induced BM-FPC trans-differentiation was significantly reduced by recombinant IL10 treatment. These results suggest that in addition to reducing mobilization of BM-FPCs, IL10 inhibits trans-differentiation of BM-FPC to myoFB and associated fibrotic signaling. TGFβ drives the fibrotic process by binding to the heterodimeric membrane receptor, which results in phosphorylation and subsequent nuclear translocation of the SMAD family of transcription factors. Thus, inhibition of the specific cellular receptors, kinases and other mediators involved in activation of the TGFβ pathway may provide effective therapeutic targets for treating cardiac fibrosis[45, 46]. Impedance of cellular differentiation and Smad2/3 phosphorylation by IL10 suggests that IL10 holds pertinent therapeutic potential for treatment of heart failure by its strong inhibitory role in BM-FPC-mediated fibrosis in pressure-overloaded myocardium. To this point, our data show that reduced recruitment of BM-FPCs in IL10 KO chimeric mice partially inhibited myocardial fibrosis and improved heart function after TAC compared to that observed in IL10KO mice.

The etiology of the fibrogenic cardiac phenotype is still being elucidated, but recent studies have demonstrated that in addition to canonical TGFβ fibrotic signaling molecules, several miRNAs contribute to myocardial fibrosis in the pressure-overloaded myocardium [25, 26, 47]. In vivo silencing of miR-21 suppresses ERK-MAP kinase fibrotic signaling and prevents cardiac dysfunction in a mouse pressure-overload-induced disease model. miR-21 regulates fibroblast survival and growth factor secretion that ultimately control the extent of interstitial fibrosis and cardiac hypertrophy [30]. To understand the underlying mechanisms by which IL10 alters TGFβ-induced BM-FPCs trans-differentiation, we assayed miRNAs expression using a commercially available fibrotic miRNAs array platform in WT or IL10 KO BM-FPC at basal level. Interestingly, the expression of most profibrotic miRNAs was increased in IL10KO BM-FPC as compared to WT BM-FPC. Among the levels of all miRNAs tested, miRNA-21 was highly upregulated in IL10KO FPC. Previous studies have shown that biogenesis of miRNA-21 is regulated by TGFβ-Smad signaling in smooth muscle cells [28, 29]. The biogenesis of miRNA-21 is tightly regulated by DROSHA. Davis et al has shown that TGFβ-Smad signaling is important for DROSHA-mediated miRNA-21maturation [28, 29]. Here, our data suggest that IL10 inhibits TGFβ-induced Smad2/3 activation. We also present here that IL10 treatment significantly inhibits TGFβ-induced miRNA-21 expression. We further validated these data by overexpressing miRNA-21 using a mimic in WT BM-FPC before IL10 and TGFβ treatment. miRNA-21 mimic treatment attenuated the inhibitory effect of IL10 on fibrosis-associated gene expression in BM-FPCs. Thus, we speculated that the IL10-mediated reduction in TGFβ-Smad2/3 signaling in this study may regulate the DROSHA protein levels and ultimately control miRNA-21 levels in activated BM-FPCs (Figure. 8F). This possibility warrants thorough investigation in future studies.

In conclusion, here we demonstrated for the first time that BM-fibroblast progenitor cells play an important role during pressure overload-induced cardiac fibrosis. IL10 negatively regulates the TAC-induced BM-FPC recruitment to the heart. We also show that in addition to reduced BM-FPC homing, IL10 changes the microenvironment of the heart and thus inhibits BM-FPC activation. At molecular level, IL10 via TGFβ-Smad signaling mechanism might modulate the miR-21 maturation process and therefore inhibits pressure overload-induced cardiac fibrosis. As bone marrow fibroblast progenitor cells are involved in cardiac fibrosis only during pathological stress, selective inhibition of their homing to the heart and of fibrotic signaling using IL10 might inhibit transition of physiological hypertrophy to heart failure and may be a potential therapeutic strategy to treat or prevent development of heart disease. A model showing the possible mechanism of IL10 mediated inhibition of TAC-induced cardiac fibrosis is shown in Figure 8F.

Supplementary Material

Refer to Web version on PubMed Central for supplementary material.

Acknowledgments

Source of Funding: Work described in this manuscript was in part supported by NIH grants HL091983, HL126186, HL053354 (to R.K.) and HL135060 (to S.K.V.); American Heart Association-Scientist Development Grant 14SDG20480104 (to S.K.V.), American Heart Association-Postdoctoral Fellowship 15POST22720022 (to

V.N.S.G.), American Heart Association-Predoctoral Fellowship 17PRE33370001 (Y.Y.) and American Heart Association-Grant-in-Aid 17GIA (D.A.G.).

References

1. Mozaffarian D, Benjamin EJ, Go AS, Arnett DK, Blaha MJ, Cushman M, Das SR, de Ferranti S, Despres JP, Fullerton HJ, Howard VJ, Huffman MD, Isasi CR, Jimenez MC, Judd SE, Kissela BM, Lichtman JH, Lisabeth LD, Liu S, Mackey RH, Magid DJ, McGuire DK, Mohler ER 3rd, Moy CS, Muntner P, Mussolino ME, Nasir K, Neumar RW, Nichol G, Palaniappan L, Pandey DK, Reeves MJ, Rodriguez CJ, Rosamond W, Sorlie PD, Stein J, Towfighi A, Turan TN, Virani SS, Woo D, Yeh RW, Turner MB. Writing Group M; American Heart Association Statistics C, Stroke Statistics S. Heart disease and stroke statistics-2016 update: A report from the american heart association. Circulation. 2016; 133:e38–360. [PubMed: 26673558]
2. Heidenreich PA, Trogdon JG, Khavjou OA, Butler J, Dracup K, Ezekowitz MD, Finkelstein EA, Hong Y, Johnston SC, Khera A, Lloyd-Jones DM, Nelson SA, Nichol G, Orenstein D, Wilson PW, Woo YJ. American Heart Association Advocacy Coordinating C, Stroke C, Council on Cardiovascular R, Intervention, Council on Clinical C, Council on E, Prevention, Council on A, Thrombosis, Vascular B, Council on C, Critical C, Perioperative, Resuscitation, Council on Cardiovascular N, Council on the Kidney in Cardiovascular D, Council on Cardiovascular S, Anesthesia, Interdisciplinary Council on Quality of C, Outcomes R. Forecasting the future of cardiovascular disease in the united states: A policy statement from the american heart association. Circulation. 2011; 123:933–944. [PubMed: 21262990]
3. Davis J, Molkentin JD. Myofibroblasts: Trust your heart and let fate decide. J Mol Cell Cardiol. 2014; 70:9–18. [PubMed: 24189039]
4. Souders CA, Bowers SL, Baudino TA. Cardiac fibroblast: The renaissance cell. Circ Res. 2009; 105:1164–1176. [PubMed: 19959782]
5. Kaur H, Takefuji M, Ngai CY, Carvalho J, Bayer J, Wietelmann A, Poetsch A, Hoelper S, Conway SJ, Mollmann H, Looso M, Troidl C, Offermanns S, Wettschureck N. Targeted ablation of periostin-expressing activated fibroblasts prevents adverse cardiac remodeling in mice. Circ Res. 2016; 118:1906–1917. [PubMed: 27140435]
6. McAnulty RJ. Fibroblasts and myofibroblasts: Their source, function and role in disease. Int J Biochem Cell Biol. 2007; 39:666–671. [PubMed: 17196874]
7. Zeisberg M, Kalluri R. Cellular mechanisms of tissue fibrosis. 1. Common and organ-specific mechanisms associated with tissue fibrosis. Am J Physiol Cell Physiol. 2013; 304:C216–C225. [PubMed: 23255577]
8. Valiente-Alandi I, Schafer AE, Blaxall BC. Extracellular matrix-mediated cellular communication in the heart. J Mol Cell Cardiol. 2016; 91:228–237. [PubMed: 26778458]
9. Fan D, Takawale A, Lee J, Kassiri Z. Cardiac fibroblasts, fibrosis and extracellular matrix remodeling in heart disease. Fibrogenesis Tissue Repair. 2012; 5:15. [PubMed: 22943504]
10. Mikawa T, Gourdie RG. Pericardial mesoderm generates a population of coronary smooth muscle cells migrating into the heart along with ingrowth of the epicardial organ. Dev Biol. 1996; 174:221–232. [PubMed: 8631495]
11. Fang M, Xiang FL, Braitsch CM, Yutzey KE. Epicardium-derived fibroblasts in heart development and disease. J Mol Cell Cardiol. 2016; 91:23–27. [PubMed: 26718723]
12. Vasquez C, Morley GE. The origin and arrhythmogenic potential of fibroblasts in cardiac disease. J Cardiovasc Transl Res. 2012; 5:760–767. [PubMed: 22987310]
13. Barisic-Dujmovic T, Boban I, Clark SH. Fibroblasts/myofibroblasts that participate in cutaneous wound healing are not derived from circulating progenitor cells. J Cell Physiol. 2010; 222:703–712. [PubMed: 20020505]
14. Carlson S, Trial J, Soeller C, Entman ML. Cardiac mesenchymal stem cells contribute to scar formation after myocardial infarction. Cardiovasc Res. 2011; 91:99–107. [PubMed: 21357194]
15. Kania G, Blyszczuk P, Stein S, Valaperti A, Germano D, Dirnhofer S, Hunziker L, Matter CM, Eriksson U. Heart-infiltrating prominin-1+/cd133+ progenitor cells represent the cellular source of transforming growth factor beta-mediated cardiac fibrosis in experimental autoimmune myocarditis. Circ Res. 2009; 105:462–470. [PubMed: 19628793]

16. Zeisberg EM, Kalluri R. Origins of cardiac fibroblasts. Circ Res. 2010; 107:1304–1312. [PubMed: 21106947]
17. Chu PY, Walder K, Horlock D, Williams D, Nelson E, Byrne M, Jandeleit-Dahm K, Zimmet P, Kaye DM. Cxcr4 antagonism attenuates the development of diabetic cardiac fibrosis. PLoS One. 2015; 10:e0133616. [PubMed: 26214690]
18. Zeisberg EM, Tarnavski O, Zeisberg M, Dorfman AL, McMullen JR, Gustafsson E, Chandraker A, Yuan X, Pu WT, Roberts AB, Neilson EG, Sayegh MH, Izumo S, Kalluri R. Endothelial-to-mesenchymal transition contributes to cardiac fibrosis. Nat Med. 2007; 13:952–961. [PubMed: 17660828]
19. Bourdreux Y, Lemetais A, Urban D, Beau JM. Iron(iii) chloride-tandem catalysis for a one-pot regioselective protection of glycopyranosides. Chem Commun (Camb). 2011; 47:2146–2148. [PubMed: 21206947]
20. Kania G, Blyszczuk P, Valaperti A, Dieterle T, Leimenstoll B, Dirnhofer S, Zulewski H, Eriksson U. Prominin-1+/cd133+ bone marrow-derived heart-resident cells suppress experimental autoimmune myocarditis. Cardiovasc Res. 2008; 80:236–245. [PubMed: 18621802]
21. Sopel MJ, Rosin NL, Lee TD, Legare JF. Myocardial fibrosis in response to angiotensin ii is preceded by the recruitment of mesenchymal progenitor cells. Lab Invest. 2011; 91:565–578. [PubMed: 21116240]
22. Pichler M, Rainer PP, Schauer S, Hoefler G. Cardiac fibrosis in human transplanted hearts is mainly driven by cells of intracardiac origin. J Am Coll Cardiol. 2012; 59:1008–1016. [PubMed: 22402073]
23. Moore-Morris T, Guimaraes-Camboa N, Banerjee I, Zambon AC, Kisseleva T, Velayoudon A, Stallcup WB, Gu Y, Dalton ND, Cedenilla M, Gomez-Amaro R, Zhou B, Brenner DA, Peterson KL, Chen J, Evans SM. Resident fibroblast lineages mediate pressure overload-induced cardiac fibrosis. J Clin Invest. 2014; 124:2921–2934. [PubMed: 24937432]
24. Travers JG, Kamal FA, Robbins J, Yutzey KE, Blaxall BC. Cardiac fibrosis: The fibroblast awakens. Circ Res. 2016; 118:1021–1040. [PubMed: 26987915]
25. van Rooij E, Olson EN. Micrornas: Powerful new regulators of heart disease and provocative therapeutic targets. J Clin Invest. 2007; 117:2369–2376. [PubMed: 17786230]
26. Thum T. Noncoding rnas and myocardial fibrosis. Nat Rev Cardiol. 2014; 11:655–663. [PubMed: 25200283]
27. Piccoli MT, Bar C, Thum T. Non-coding rnas as modulators of the cardiac fibroblast phenotype. J Mol Cell Cardiol. 2016; 92:75–81. [PubMed: 26764220]
28. Davis BN, Hilyard AC, Lagna G, Hata A. Smad proteins control drosha-mediated microrna maturation. Nature. 2008; 454:56–61. [PubMed: 18548003]
29. Blahna MT, Hata A. Smad-mediated regulation of microrna biosynthesis. FEBS Lett. 2012; 586:1906–1912. [PubMed: 22306316]
30. Thum T, Gross C, Fiedler J, Fischer T, Kissler S, Bussen M, Galuppo P, Just S, Rottbauer W, Frantz S, Castoldi M, Soutschek J, Koteliansky V, Rosenwald A, Basson MA, Licht JD, Pena JT, Rouhanifard SH, Muckenthaler MU, Tuschl T, Martin GR, Bauersachs J, Engelhardt S. Microrna-21 contributes to myocardial disease by stimulating map kinase signalling in fibroblasts. Nature. 2008; 456:980–984. [PubMed: 19043405]
31. Wang J, Liew OW, Richards AM, Chen YT. Overview of micrornas in cardiac hypertrophy, fibrosis, and apoptosis. Int J Mol Sci. 2016; 17:749.
32. Verma SK, Krishnamurthy P, Barefield D, Singh N, Gupta R, Lambers E, Thal M, Mackie A, Hoxha E, Ramirez V, Qin G, Sadayappan S, Ghosh AK, Kishore R. Interleukin-10 treatment attenuates pressure overload-induced hypertrophic remodeling and improves heart function via signal transducers and activators of transcription 3-dependent inhibition of nuclear factor-kappab. Circulation. 2012; 126:418–429. [PubMed: 22705886]
33. Yip HK, Youssef AA, Chang LT, Yang CH, Sheu JJ, Chua S, Yeh KH, Lee FY, Wu CJ, Hang CL. Association of interleukin-10 level with increased 30-day mortality in patients with st-segment elevation acute myocardial infarction undergoing primary coronary intervention. Circ J. 2007; 71:1086–1091. [PubMed: 17587715]

34. Krishnamurthy P, Thal M, Verma S, Hoxha E, Lambers E, Ramirez V, Qin G, Losordo D, Kishore R. Interleukin-10 deficiency impairs bone marrow-derived endothelial progenitor cell survival and function in ischemic myocardium. Circ Res. 2011; 109:1280–1289. [PubMed: 21959218]
35. Garikipati VN, Krishnamurthy P, Verma SK, Khan M, Abramova T, Mackie AR, Qin G, Benedict C, Nickoloff E, Johnson J, Gao E, Losordo DW, Houser SR, Koch WJ, Kishore R. Negative regulation of mir-375 by interleukin-10 enhances bone marrow-derived progenitor cell-mediated myocardial repair and function after myocardial infarction. Stem Cells. 2015; 33:3519–3529. [PubMed: 26235810]
36. Nagpal V, Rai R, Place AT, Murphy SB, Verma SK, Ghosh AK, Vaughan DE. Mir-125b is critical for fibroblast-to-myofibroblast transition and cardiac fibrosis. Circulation. 2016; 133:291–301. [PubMed: 26585673]
37. Krishnamurthy P, Lambers E, Verma S, Thorne T, Qin G, Losordo DW, Kishore R. Myocardial knockdown of mrna-stabilizing protein hur attenuates post-mi inflammatory response and left ventricular dysfunction in il-10-null mice. FASEB J. 2010; 24:2484–2494. [PubMed: 20219984]
38. Kishore R, Krishnamurthy P, Garikipati VN, Benedict C, Nickoloff E, Khan M, Johnson J, Gumpert AM, Koch WJ, Verma SK. Interleukin-10 inhibits chronic angiotensin ii-induced pathological autophagy. J Mol Cell Cardiol. 2015; 89:203–213. [PubMed: 26549357]
39. Verma SK, Lal H, Golden HB, Gerilechaogetu F, Smith M, Guleria RS, Foster DM, Lu G, Dostal DE. Rac1 and rhoa differentially regulate angiotensinogen gene expression in stretched cardiac fibroblasts. Cardiovasc Res. 2011; 90:88–96. [PubMed: 21131638]
40. Tarzami ST. Chemokines and inflammation in heart disease: Adaptive or maladaptive? Int J Clin Exp Med. 2011; 4:74–80. [PubMed: 21394288]
41. Gong Y, Zhao Y, Li Y, Fan Y, Hoover-Plow J. Plasminogen regulates cardiac repair after myocardial infarction through its noncanonical function in stem cell homing to the infarcted heart. J Am Coll Cardiol. 2014; 63:2862–2872. [PubMed: 24681141]
42. Sun M, Dawood F, Wen WH, Chen M, Dixon I, Kirshenbaum LA, Liu PP. Excessive tumor necrosis factor activation after infarction contributes to susceptibility of myocardial rupture and left ventricular dysfunction. Circulation. 2004; 110:3221–3228. [PubMed: 15533863]
43. Huber BC, Beetz NL, Laskowski A, Ziegler T, Grabmaier U, Kupatt C, Herbach N, Wanke R, Franz WM, Massberg S, Brunner S. Attenuation of cardiac hypertrophy by g-csf is associated with enhanced migration of bone marrow-derived cells. J Cell Mol Med. 2015; 19:1033–1041. [PubMed: 25754690]
44. Dobaczewski M, Chen W, Frangogiannis NG. Transforming growth factor (tgf)-beta signaling in cardiac remodeling. J Mol Cell Cardiol. 2011; 51:600–606. [PubMed: 21059352]
45. Stratton MS, McKinsey TA. Epigenetic regulation of cardiac fibrosis. J Mol Cell Cardiol. 2016; 92:206–213. [PubMed: 26876451]
46. Yu LM, Xu Y. Epigenetic regulation in cardiac fibrosis. World J Cardiol. 2015; 7:784–791. [PubMed: 26635926]
47. Creemers EE, van Rooij E. Function and therapeutic potential of non-coding rnas in cardiac fibrosis. Circ Res. 2016; 118:108–118. [PubMed: 26538569]

Clinical Perspective

What is New?

- Despite significant progress made to identify molecular mechanisms that contribute to cardiac fibrosis over the past decades, its mechanistic basis is still not well understood.
- This study demonstrates that in addition to resident cardiac fibroblasts, bone marrow-derived myofibroblasts significantly contribute to progression of pathological cardiac fibrosis, and that pleotropic anti-inflammatory cytokine IL10 inhibits the recruitment and trans-differentiation of BM-FPCs into the pressure-overloaded myocardium.
- At molecular level, we show that IL10 noticeably inhibits TGFβ-Smad2/3 signaling in activated BM-FPCs.
- We discover that inhibition of TGFβ-Smad2/3 signaling-mediated miRNA-21 maturation as a novel mechanism by which IL10 inhibits BM-FPC-mediated cardiac fibrosis in the pressure-overloaded myocardium.

What are the clinical Implications?

- Left ventricular hypertrophy accompanied by myocardial fibrosis contributes for heart failure, but no medical therapies particularly effective for retarding or reversing this maladaptive process.
- The results presented in this study have important clinical implications because bone marrow cells are involved in cardiac fibrosis only during pathological stress.
- Thus, selective inhibition of their homing to the heart and of fibrotic signaling using IL10 or selective miRNAs might inhibit transition of physiological hypertrophy to heart failure and may be a potential therapeutic strategy to treat or prevent the development of hypertrophic remodeling in heart failure patients.

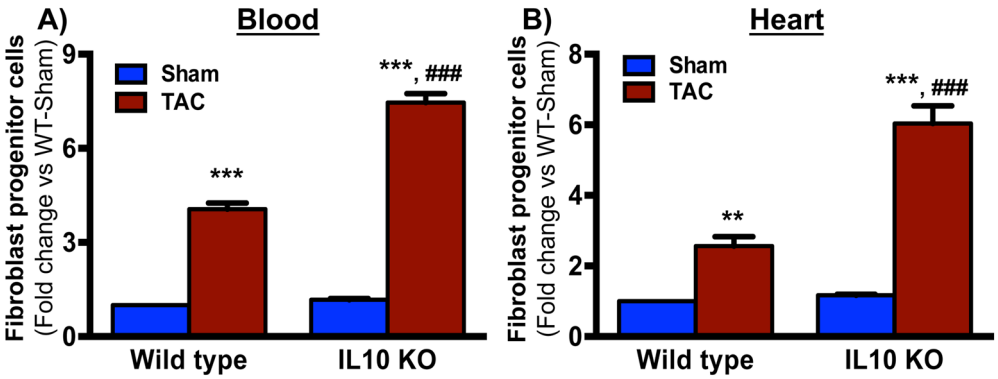

Fig. 1. TAC-induced BM-FPC mobilization from bone marrow into blood and homing to the heart

Five days after TAC surgery peripheral blood **(A)** and heart **(B)** were collected from WT and IL10 KO mice and processed to measure the fibroblast progenitor cell mobilization and recruitment by FACS. TAC-induced homing of BM-FPCs was exaggerated in IL10KO mice. **p<0.01, ***p<0.001 vs sham, ###p<0.001 vs TAC. BM-FPCs are Lin^{-} $CD45^{+}$, prominin 1^{+} cells and FITC and PE conjugated antibodies were used for FACS analysis respectively. Two-way ANOVA using Tukey-Kramer multiple comparisons post-hoc test was used to determined the significant difference between genotypes and surgeries (N=6–10)

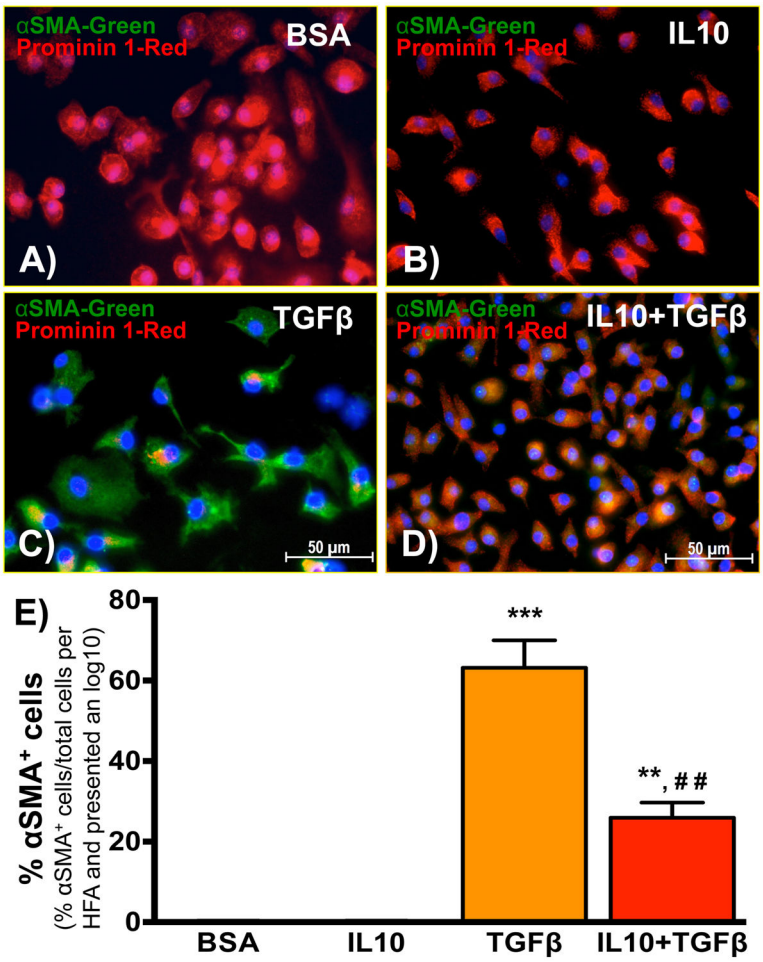

Fig. 2. IL10 inhibits TGFβ-induced trans-differentiation of BM-FPCs to myoFBs

(A–D) BM-FPCs were treated with IL10 and/or TGFβ for 48 hr in serum-free IMDM media. After treatment, BM-FPCs were washed with PBS, fixed in PFA and permeabilized using Triton® 100. After blocking, cells were incubated with primary and secondary antibodies. DAPI was used to stain the nucleus. **(E)** Quantitative analysis suggests that IL10 treatment significantly inhibited TGFβ-induced trans-differentiation of BM-FPCs to myofibroblasts, evident in the paucity of SMA^+ cells. Red= Prominin 1, Green= αSMA and blue= DAPI. The original magnification was 400X. ***p<0.001, **p<0.01 vs. BSA; $^{\#\#}$p<0.01 vs. TGFβ. (N=6) HFA= high field area.

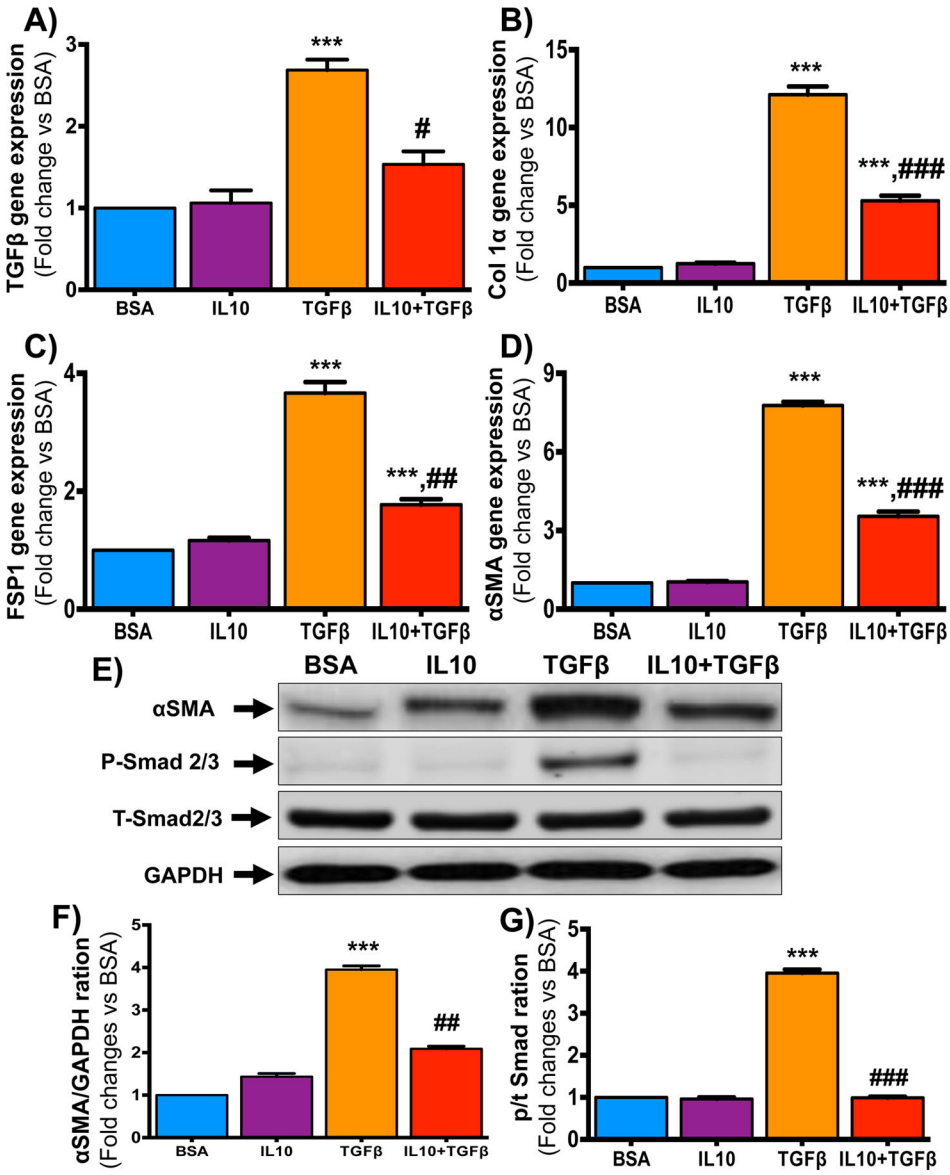

Fig. 3. IL10 attenuates TGFβ-induced fibrotic signaling in BM-FPCs

(A–C) BM-FPCs were treated with IL10 (24 hr), TGFβ (6 hr for protein and 24 hr for RNA analysis), or both, in serum free medium. Total RNA was isolated 24 hours after treatment. Gene expression levels of fibrosis-associated genes were measured using specific primers and probes. RT-PCR data showed that IL10 inhibits TGFβ-induced **(A)** TGFβ, **(B)** collagen 1α, **(C)** FSP-1 and **(D)** αSMA genes expression. **(E–G)** Western blots of total cell lysates show Smad2/3 phosphorylation and total αSMA levels 6 hours after IL10 and TGFβ treatments. Respective total SMAD and GAPDH were used as loading controls. Bar graphs show fold- changes in **(E and F)** αSMA levels and **(E and G)** Smad2/3 phosphorylation. IL10 treatment attenuated TGFβ signaling, an indicator of BM-FPC activation. ***p<0.001 vs. BSA; $^{\#}$p<0.05, $^{\#\#}$p<0.01, $^{\#\#\#}$p<0.001 vs. TGFβ. (N=6)

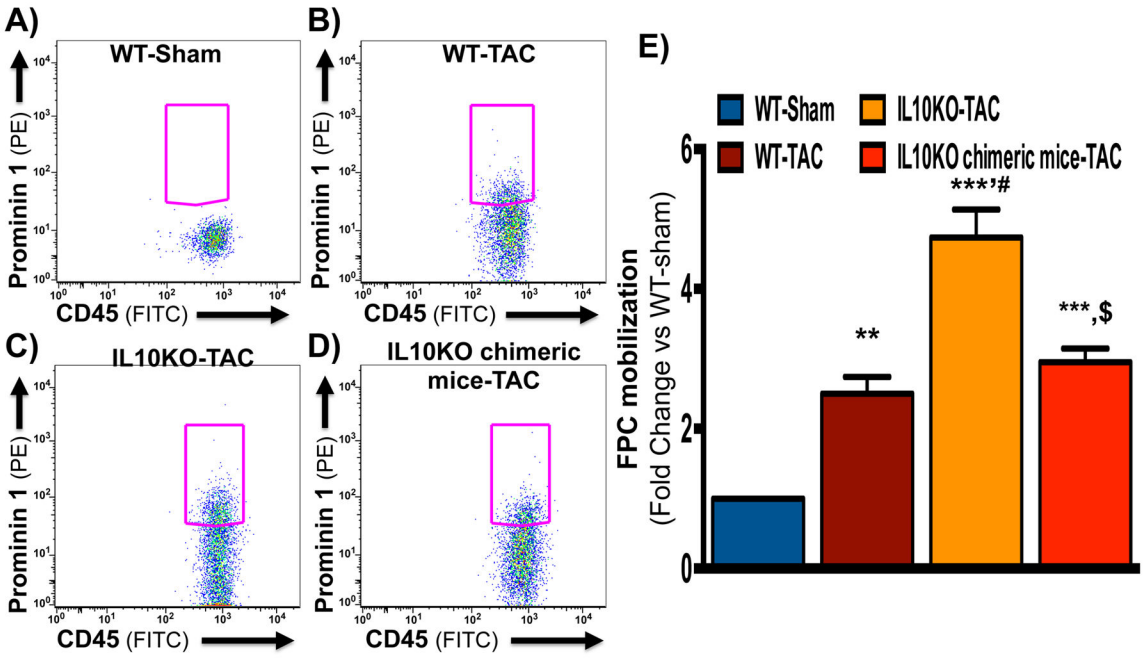

Fig. 4. FACS analysis of peripheral mononuclear cells for TAC-induced BM-FPCs mobilization in BMT mice

Five days after TAC surgery, peripheral blood was collected from WT, IL10KO and IL10KO chimeric mice by tail vein bleeding and analyzed for CD45 and prominin 1 expressing cells to measure the mobilization of BM-FPCs by FACs. **(A–C and E)** BM-FPCs were significantly increased in IL10KO mice peripheral blood compared to WT mice after TAC. **(D–E)** WT bone marrow reconstitution in chimeric mice significantly reduced BM-FPC mobilization. **p<0.01, ***p<0.001 vs. WT-Sham; $^{\#}$p<0.05 vs. WT-TAC; $^{\$}$p<0.05, vs. IL10KO-TAC. PE: phycoerythrin; FITC: Fluorescein isothiocyanate. (N=8)

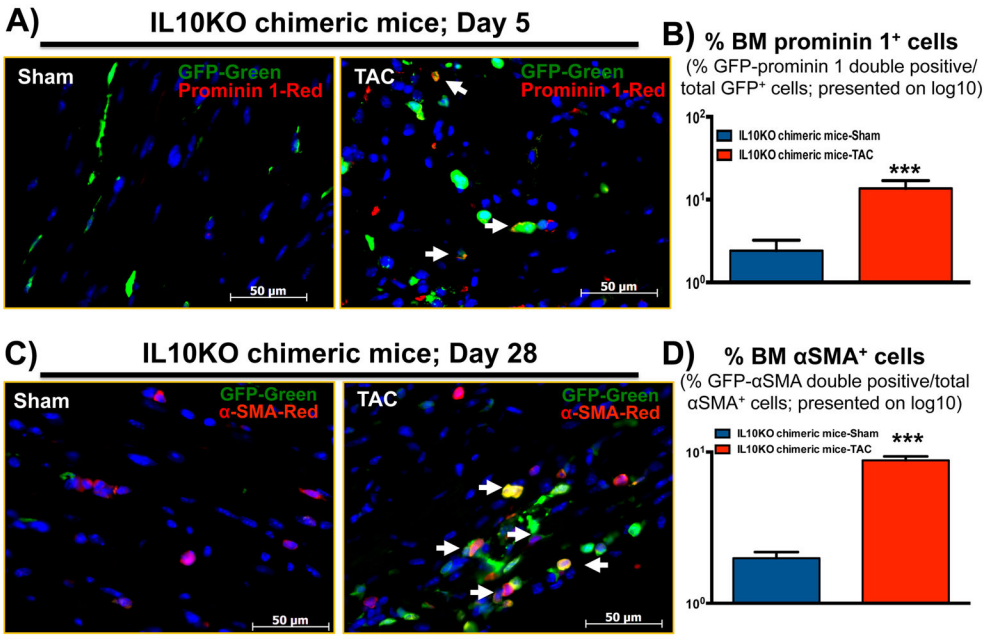

Fig. 5. Donor bone marrow fibroblast progenitor cells contribute to myoFBs after TAC surgery

Hearts from chimeric mice were perfused with PBS, fixed in formalin and embedded in paraffin. **(A)** 5 days after TAC surgery, heart sections were immunostained with GFP and prominin 1 antibodies. **(B)** The number of bone marrow derived-prominin 1 positive cells was increased in hearts after TAC surgery. **(C)** To assess bone marrow-derived myofibroblasts in heart, 28 days after TAC, heart sections were immunostained with GFP (for bone marrow origin) and α-smooth muscle actin (myoFB marker). **(D)** The increased number of double-positive bone marrow-derived myofibroblasts (yellow) was seen in IL10KO chimeric mouse hearts. Green-GFP, Red- prominin 1 **(A)** or α-SMA **(C)** and blue-DAPI. The original magnification was 400X. The quantitative data are presented on log10 scale value. ***p<001 vs chimeric mice sham group. IL10KO chimeric mice: IL10 knockout mice with WT mice bone marrow transplantation. (N=6).

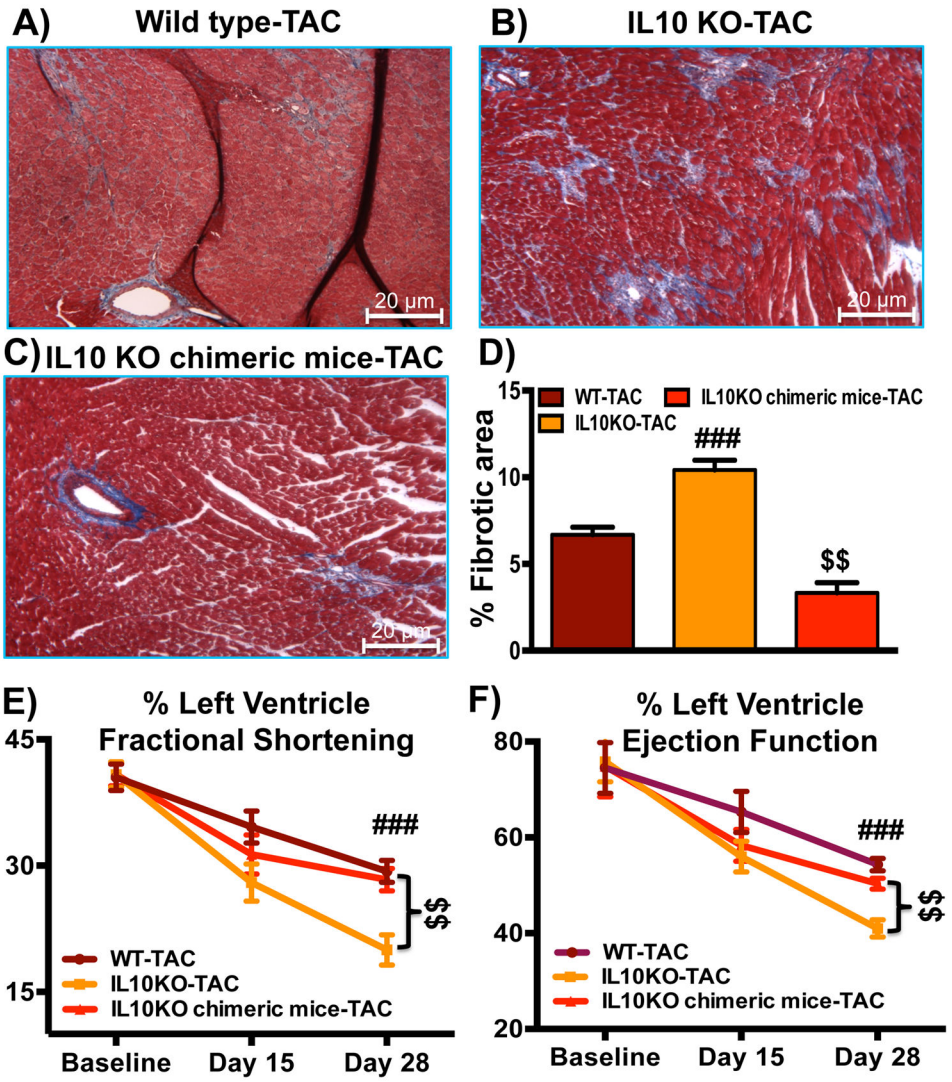

Fig. 6. Wild type bone marrow reconstitution in IL10 KO mice inhibits TAC-induced myocardial fibrosis and improves cardiac function

Pressure overload was induced in WT, IL10KO and IL10KO chimeric mice. After cardiac function measurement, hearts were perfused and fixed in formalin. Masson's trichrome staining was performed on paraffin-embedded left ventricular sections to reveal collagen deposition (blue). (**A, B and D)** IL10KO mice showed exaggerated fibrosis compared to WT mice 28 days post-surgery. **(C,D)** TAC-induced fibrosis in IL10KO mice was partially reduced in IL10KO chimeric mice. The original magnification was 200× (N=6). **(E–F)** The reconstitution of WT bone marrow cells in IL10KO mice resulted in improved cardiac function as measured by M-mode echocardiography. $^{###}$p<0.001 vs. WT-TAC; $^{\$\$}$p<0.01 vs. IL10KO-TAC. IL10KO chimeric mice: IL10 knockout mice with WT mice bone marrow transplantation. (N=10)

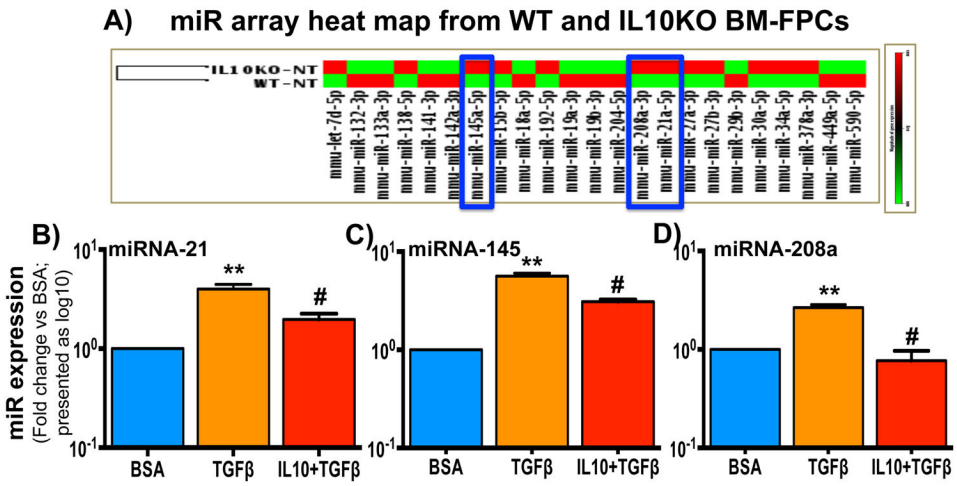

Fig. 7. IL10 KO mice bone marrow-derived FPCs showed enhanced expression of profibrotic miRNAs

Total RNA was isolated from WT and IL10KO mice BM-FPCs using miRNeasy kit (Qiagen) and fibrosis-associated miRNA platform was used to assess the miRNAs level using Taqman microRNA assay. **(A)** At basal level fibrosis-associated miRNAs expression was significantly increased in IL10KO BM-FPCs compared to WT BM-FPCs with maximum expression of miRNA21, 145 and 208a (N=6). **(B–D)** miRNA21/145/208a expression was measured in WT-FPCs treated with IL10 and TGFβ by RT-PCR. IL10 treatment significantly inhibits TGFβ-induced miRNA-21, -145 and 208a expression. **$p<0.01 vs BSA, #$p<0.05 vs TGFβ. IL10KO mice: IL10 Knockout mice; BM-FPC: Bone marrow fibroblast progenitor cells. (N=6)

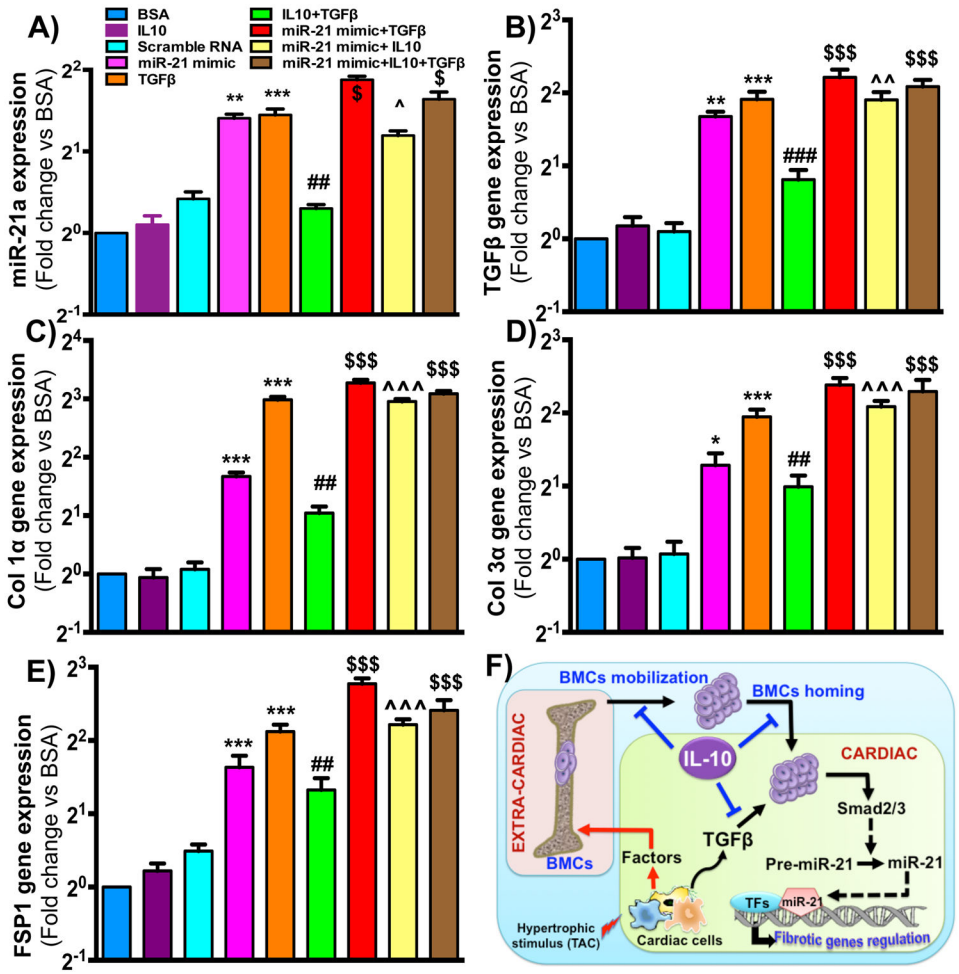

Fig. 8. miR-21 overexpression attenuates IL10 effect on TGFβ-induced fibrosis-associated genes expression in WT BM-FPCs

BM-FPCs were transfected with miRNA-21 mimic for 12 hours using lipofectamine 2000 transfection reagent before IL10 and TGFβ treatments and miRNA-21 expression was measured by RT-PCR. **(A)** miRNA-21 mimic transfection significantly increased miRNA-21 expression in BM-FPCs. **(B–E)** 24 hrs after mimic, IL10 and TGFβ treatments, cells were harvested to measured the expression of fibrosis marker genes by RT-PCR. Relative levels of target genes expression were normalized with 18S. IL10 significantly inhibited TGFβ-induced fibrosis-associated genes expression. Restoration of miRNA-21 expression using miRNA-21 mimic significantly attenuated the IL10 effect on expression of these genes. ***p<0.001, **p<0.01, *p<0.05 vs BSA, ###p<0.001, ##p<0.01 vs TGFβ; $$$p<0.001, $p<0.05 vs TGFβ and ^^^p<0.001, ^^p<0.01, ^p<0.05 vs miR-21 mimic alone. (N=6) **(F)** Schematic diagram indicates TAC-induced mobilization and homing of BM-FPCs to the heart. In the heart, profibrotic stimuli (TGFβ in this case) first facilitates BM-FPC activation to myofibroblasts and then promote Smad2/3 dependent miRNA-21 maturation. The miRNA-21 maturation ultimately leads to fibrotic gene activation in activated myofibroblasts. On the other hand, IL10 inhibits TAC-induced mobilization,

homing and activation of these cells and regulates cardiac fibrosis. Factor: Chemokine/cytokines; BMCs: Bone marrow cells; IL10 Interleukin-10.